Second International Conference on CFD in the Minerals and Process Industries
CSIRO, Melbourne, Australia
6-8 December 1999

THE EFFECT OF PARTICLE SHAPE ON HOPPER DISCHARGE

Paul W. CLEARY

CSIRO Mathematical and Information Sciences, Clayton, Victoria 3169, AUSTRALIA

ABSTRACT

Hopper flows are an important class of industrial particle flows. The inclusion of particle shape allows DEM models to replicate many features of real hopper flows that are not possible when using circular particles. Elongated particles can produce flow rates up to 30% lower than for circular particles and the flow patterns are quite different. The yielding of the particle microstructure resembles more the tearing of a continuum solid, with large scale quasi-stable voids being formed and large groups of particles moving together. The flow becomes increasingly concentrated in a relatively narrow funnel above the hopper opening. This is encouragement that DEM may be able to predict important problems such as bridging and rat-holing. Increasing the blockiness or angularity of the particles also increases resistance to flow and reduces flow rates by up to 28%, but does not have any perceptible effect on the nature of the flow.

INTRODUCTION

The flow of particulate material from hoppers has been a popular modelling problem for many years. The relatively simple geometry and well-defined flow pattern has made it attractive for both discrete element and continuum modellers (Holst et al., 1997). Whilst both can qualitatively predict mass flow, neither method has been able to predict funnel flow and phenomena such as rat-holing.

Generally the averaging used to produce the continuum equations and the lack of information needed for the complex constitutive laws means that discontinuous flow behaviour is difficult to predict. Conversely, most discrete element modelling has been two dimensional and uses mono-disperse or slightly poly-disperse distributions of discs. The flows predicted are generally far too fluid with the flow near the side walls being too rapid.

The two essential aspects that have been neglected in DEM models are the effect of particle shape and inter-particle cohesion. Both contribute significantly to the shear strength of the granular assembly and determine where the material will fail and flow and when it will remain stationary. As a first step towards developing realistic hopper flow modelling, a study of the effect of particle shape on the flow behaviour in a two-dimensional hopper is presented. The change in flow pattern, discharge mass flow rate, discharge velocity and wall forces with the blockiness and aspect ratio of the particles are described.

THE DISCRETE ELEMENT SIMULATION METHOD

Discrete element modelling (DEM) of granular flows involves following the trajectories, spins and orientations of all the particles and predicting their interactions with other particles and with their environment. These methods are now well established and are described in review articles by Campbell (1990), Barker (1994) and Walton (1994). DEM has been successfully applied to many industrial and mining applications, such as dragline excavators (Cleary, 1998a), ball mills (Mishra and Rajamani 1992, 1994, Cleary 1998b) and for a wide selection of industrial applications in Cleary (1998c).

In the two dimensional simulations described here the hoppers are constructed from linear segments. The particles are modelled as either discs or super-quadrics whose general form

$$x^N + \left(\frac{y}{A}\right)^N = s^N \ ,$$

is used to describe non-circular particles, where the power N determines the blockiness of the particle (with the shape smoothly changing from a circle to a square as N increases) and A is the aspect ratio of the particle with semi-major axis s. Super-quadrics have previously been used to describe particle shapes by Williams and co-workers (see Williams and Pentland (1992) and its references). In our implementation aspect ratios of up to 20:1 and blockiness factors up to 12 have been routinely used. Using non-circular particles of any type has a number of additional costs. Some of these are generated by the increase in coordination numbers for non-circular particles, some by the more complex vectorial relationship between the normal and tangential forces and the final net cartesian forces used for particle motions, some by the integration of an additional particle orientation equation, but a large proportion by the increased demands of contact detection. For our implementation, the additional cost of the contact detection is essentially independent of both the blockiness and the aspect ratio and is approximately 45-55% of the computation time; the simulation time using super-quadrics is then between 1.9 and 2.1 times that of a similar simulation using circular particles (not N=2 super-quadrics). Overall, super-quadric particle shapes are able to capture many of the essential elements of real particle shape and greatly extend the range of applicability of DEM with only moderate computational cost. The effect of particle shape has been explored in detail for the filling of dragline buckets and mixing in slowly rotating tumblers (including encouraging validation against mixing experiments) in Cleary (1999).

The particles are allowed to overlap and the amount of overlap Δx, and normal v_n and tangential v_t relative velocities determine the collisional forces. There are a range of possible contact force models available that approximate the collision dynamics to various extents. A conventional linear spring-dashpot model is used in these simulations.

The normal force

$$F_n = -k_n \Delta x + C_n v_n \ ,$$

consists of a linear spring to provide the repulsive force and a dashpot to dissipate a proportion of the relative kinetic energy. The maximum overlap between particles is determined by the stiffness k_n of the spring in the normal direction. Typically average overlaps of 0.1-1.0% are desirable, requiring spring constants of the order of 10^6-10^7 N/m. The normal damping coefficient C_n is chosen to give a required coefficient of restitution ε (defined as the ratio of the post-collisional to pre-collisional normal component of the relative velocity), and is given in Cleary (1998c).

The tangential force is given by

$$F_t = \min\left\{\mu F_n, k_t \int v_t dt + C_t v_t\right\},$$

where the integral of the tangential velocity v_t over the collision behaves as an incremental spring (with stiffness k_t) that stores energy from the relative tangential motions and represents the elastic tangential deformation of the contacting surfaces. The dashpot (with strength C_t) dissipates energy from the tangential motion and models the tangential plastic deformation of the contact. The total tangential force (given by the sum of the elastic and plastic components) is limited by the Coulomb frictional limit at which point the surface contact shears and the particles begin to slide over each other. Here μ is the dynamic friction coefficient.

The discrete element algorithm itself is relatively simple with three essential parts:

1. A search grid is used to periodically build a particle near-neighbour interaction list. Using only particle pairs in the near neighbour list reduces the force calculation to an $O(N)$ operation, where N is the total number of particles. Industrial simulations with 100,000 particles are possible in reasonable times on current workstations.
2. The collisional forces on each of the particles and boundary objects are evaluated efficiently using the near-neighbour list and the spring-dashpot interaction model and then transformed into the simulation frame of reference.
3. All the forces on the boundary objects (such as the hopper) and the particles are summed and the resulting equations of motion are integrated. The integration scheme is a second-order predictor-corrector, with between 10 and 50 timesteps required to accurately integrate each collision. This gives very small time steps, typically 10^{-3} to 10^{-6} s, depending on the controlling length and time scales of each application.

HOPPER CONFIGURATION AND SIMULATIONS

The hopper used for this study is just over 1.5 m in height, has an internal width of 740 mm, a converging section with a 60 degree hopper half angle, and an opening for discharge with internal width of 140 mm wide. This configuration is shown in Figure 1 for the case with N=6 and A=1.0.

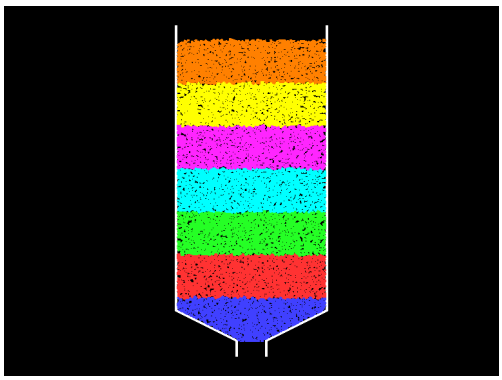

Figure 1: Configuration for hopper simulations.

The particles used have diameters uniformly distributed between 5 mm and 25 mm. The diameter of the non-circular particles is defined as the largest dimension across the particle. The coefficient of restitution used was 0.3 (appropriate for many types of rocks) and the coefficient of friction was 0.75 (appropriate for many materials with angles of internal friction of around 43 degrees).

In each case it is necessary to build a microstructure of particles with the specified shapes. For the circular particle case, microstructure is built using one of the fill algorithms in the pre-processor. For other shapes the hopper was filled to a higher level, the particle were scaled to give the appropriate aspect ratios and mapped to give the desired blockiness N and then allowed to settle under gravity. After allowing any oscillations generated by the settling to damp out, the now packed particle microstructure has particles above a height of 1.5 m (measured from the top of the discharge opening) removed and all the residual particle forces, velocities and spins are set to zero. This gives an identical volume of particles for each choice of particle shape in exactly the same starting configuration. This allows careful comparisons of the discharge flows to be made.

For each discharge simulation, the control volume is made periodic in the vertical direction. Particles that have discharged re-enter at the top of the simulation domain and fall onto the top surface of the particles. This means that the mass of material in the hopper is constant in time and gives a constant pressure head driving the flow. This produces a well-defined steady flow that readily allows comparison between cases. If this is not done then there is an approximately linear decline in the discharge mass flow rate and the wall forces have steadily declining amplitude. This would significantly complicate the interpretation of the results.

Several types of data are collected. The particles in the discharge stream are monitored and the time-varying mass flow rate and hopper discharge speed are calculated. The time series of the total force applied by the particles to the

hopper structure (in both vertical and horizontal directions) is calculated.

Three series of simulations were performed:

1. Keeping the aspect ratio constant at A=1, the blockiness was varied between 2 (circular) and 12 (very squarish).
2. Keeping the blockiness at N=2 the aspect ratio was varied from 1 down to 0.2. All these particles are elliptical.
3. Keeping the blockiness at N=10 the aspect ratio was varied from 1 down to 0.2. All these particles are essentially rectangular.

The variation of the bulk density of the particles with shape variation is of interest. Normalising the bulk densities by that of the circular particle case, reveals that any non-circularity leads to higher bulk densities. The best packing occurs for N=4. The packing slowly becomes looser with both increasing and decreasing N. For the elliptical particles, the best packing occurs for an aspect ratio of A=0.6. The packing deteriorates quickly with lower aspect ratios, with the A=0.2 case having a relative bulk density of only 0.95. This indicates that the highly elongated particles with random orientations are able to trap 5% more voids than can circular particles. For rectangular particles, the best packing occurs for the square (A=1) particles with declining bulk density thereafter. For very elongated particles (A=0.2) the bulk density is around 7% lower than for circular particles.

COMPARISON OF CIRCULAR PARTICLE FLOW TO HIGHLY NON-CIRCULAR

Figure 2 shows the start of the discharge flow, with very elongated ellipses (A=0.2) on the left and the traditional circular particles on the right. The relative rate of discharge can be judged by the movement of the interfaces between strata. Even at t=0.2 s, the deformation of the lowest interface for the elliptical particles remains highly localised directly above the exit port. In contrast, the circular particle interface is deformed across the width of the hopper forming a reasonably straight-sided V. By t=0.5 s (the last frames of Figure 2) the deformation of the interface for the elliptical particles barely exceeds the width of the opening below and the majority of the interface is undisturbed. Again in contrast, the circular particle case shows significant flow far to the sides of the exit. The interface maintains its V shape, which deepens in the centre. The circular particles in the computational model flow far too freely, giving a flow that is much closer to that of mass flow even for this very flat bottomed hopper, which would normally be expected to produce a highly concentrated funnel flow. This is unrealistic for real materials.

In addition to predicting far more localised central flow (in accordance with observation), the elliptical particles also demonstrate significant strength in resisting shear and nicely illustrate that arching stresses are being reproduced. This can be seen by close inspection of the mode of microstructure failure above the discharge port. The model shows (at t=0.2 s) the formation of an arch-like void structure directly over the exit as the lower material falls away, but the well-supported material above does not follow immediately. The highly elliptical particle shape gives the microstructure significantly more strength and greatly slows the rate of yielding and flow. In the second set of frames, the microstructure has failed higher up and another chunk of material has begun to descend. Again, this produces significant void structure above and these are arch like in shape, reflecting the well known arching stresses that support real granular materials in such situations. In the next frame, the material that had previously failed has moved downwards, but a large quasi-stable arch on the right continues to support the granular material on that side. Significant rents in the fabric of the microstructure can be seen to the left and well above the opening. These particles do not flow like discrete particles, but move much more like a fracturing continuum. In contrast, the circular particle flow is always smooth, with each particle moving independently, has negligible changes in the void structure, and barely inhibits the flow of material near the sides. The elliptical particle model thus appears to be capturing a significantly larger proportion of the hopper flow dynamics.

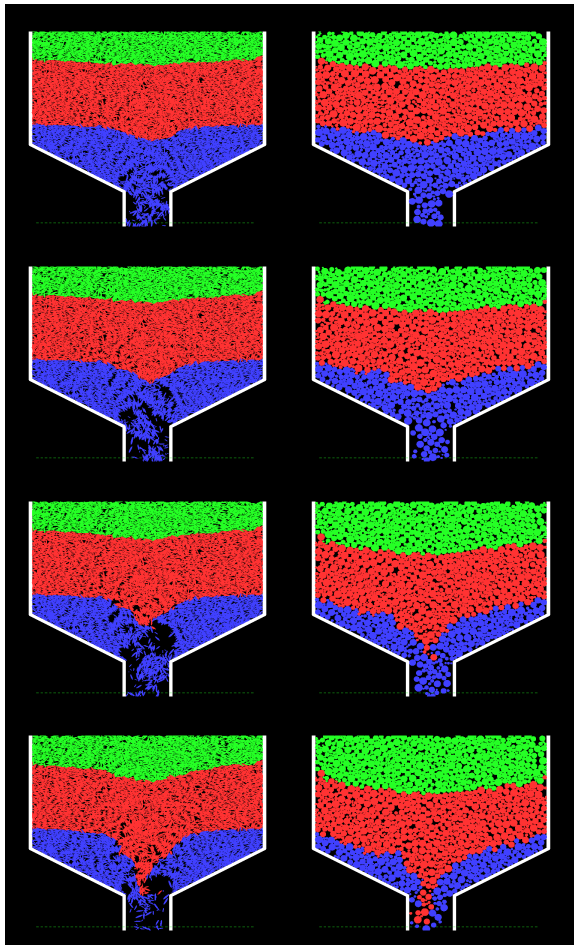

Figure 2: Flow of elongated ellipical particles with A=0.2 and N=2 (left) and circular particles (right). The top row is at t=0.2 s with each subsequent row spaced by 0.1 s.

EFFECT OF BLOCKINESS N

Figure 3 shows the effect of increasing particle blockiness (for constant aspect ratio A=1) on the flow pattern in the lower half of the hopper after 2.5 s. The deformation of the strata illustrates clearly the changes that occur. For circular particles (N=2) the flow is very free and all

particles are easily able to exit, with only those within a couple of particle diameters of the wall impeded in any way. This can be seen clearly by the sharp upturn in the interface between the yellow and purple layers (the highest interface) immediately adjacent to the walls. The yellow (lightest grey) has moved down a significant distance into the hopper. This is very close to mass flow. For N=3, the pattern is broadly similar, but the yellow material has not moved so far down into the hopper and the lighter blue material no longer reaches the opening by 2.5 s. For N=4 and all higher values, the behaviour is similar, with the yellow material travelling progressively less far down into the hopper with increasing N. The shapes of the lower interfaces are broadly unchanged, still being V like with reasonably straight sides. Each of these interfaces also moves slightly higher with each increase in N. The increasing blockiness has a distinct effect by reducing the discharge rate, but perhaps surprising does little to change the pattern of the flow, just its rate. This is quite the opposite to the findings for filling of dragline buckets (Cleary, 1999) where the blockiness was shown to have a significant effect in increasing resistance to bucket penetration.

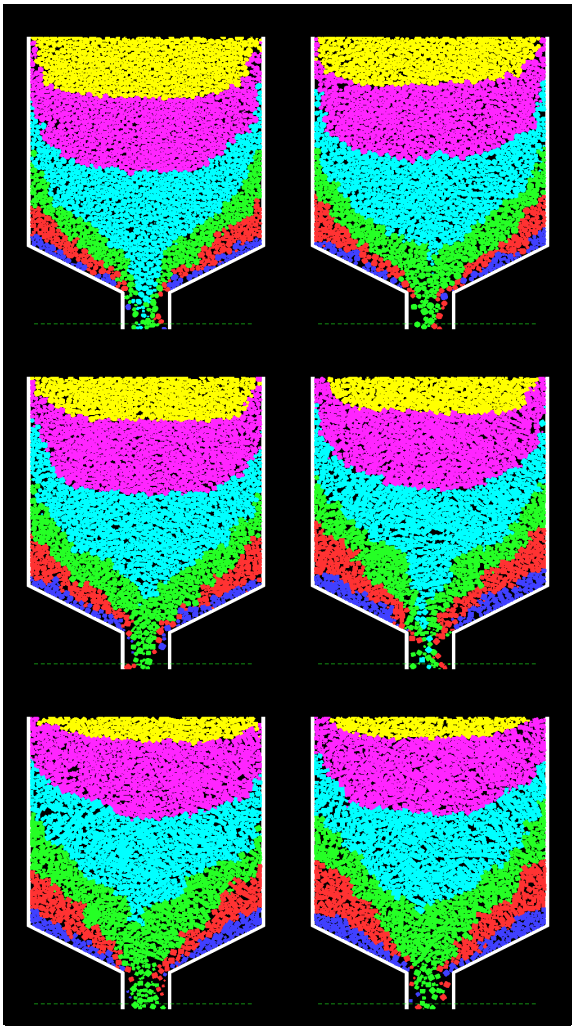

Figure 3: Discharge pattern at t=2.5 s for increasing blockiness of the particles (from top left to bottom right) N=2, N=3, N=4, N=6, N=8 and N=10.

EFFECT OF ASPECT RATIO A

Comparing the effect of varying aspect ratio for circular particles (left column of Figure 4) we find that the main effect of increasing A is to slowly increase the levels of the interfaces between colours, and more importantly, to change the shape of these interfaces. For all the previous cases the lower interfaces were V shaped with straight edges. For A=0.6 there is a hint of upward curvature in the interfaces. For A=0.4 this curvature is very clearly defined and indicates that the material strength in the side regions is now becoming strong enough to resist shear and reduce particle losses from there. Increasing aspect ratio also appears to reduce the rate of disharge slowly.

Examining the effect of increasing aspect ratio A for rectangular particles (right column of Figure 4) the same qualitative phenomena are observed, but only stronger. The flow rates are already much reduced by the blockiness of the particles for N=10 and A=1. Increasing aspect ratio progressively reduces the flow rate further, again shown by the reduced penetration of the yellow material into the hopper. More importantly, the lower V shaped interfaces again start to become curved upwards by A=0.6. In contrast to the elliptical case, the interfaces now become jagged as the yielding becomes discrete failures rather than continuous deformation. For the very elongated squarish case (A=0.2) the change in the interface structure is quite marked. They are essentially bi-linear now with a steep central section and very flat side regions. This indicates that there is barely any cumulative movement in this side material. The microstructure strength is now significant. The flow is now becoming concentrated in the central core and is approaching the flow behaviour known as rat-holing, where a narrow funnel in the centre of the hopper empties and new material flows along the top surface and down the rat-hole while all the side material remains stationary. This is an undesirable state, but it is critical that DEM models be able to predict its occurrence. Finally, significant void regions are clearly observable in this last flow-resistant case.

HOPPER DISCHARGE RATES

Figure 5 shows the average mass flow predicted for the hopper for particles with several values of blockiness. The circular particles produce the highest flow rate since they are the most free flowing. Departures from circularity produce a linear (with N) decline in the mass flow rate, until N=8 after which the subtle variations in particle shape fail to make any further difference to the nature of the flow.

Figure 6 shows the mass flow rate as a function of the aspect ratio for elliptic particles (top) and rectangular particles (lower frame). In both cases there is a linear decrease in the mass flow rate with increasing elongation of the particles. For A=0.2 the reduction is around 30%.

WALL FORCES

Figure 7a shows the time series of the total force exerted by the circular particles on the hopper. The mean value of this time series is the weight of the particles, which is around 20 kN/m. Even for circular particles there are large fluctuations which average around 50% of the mean.

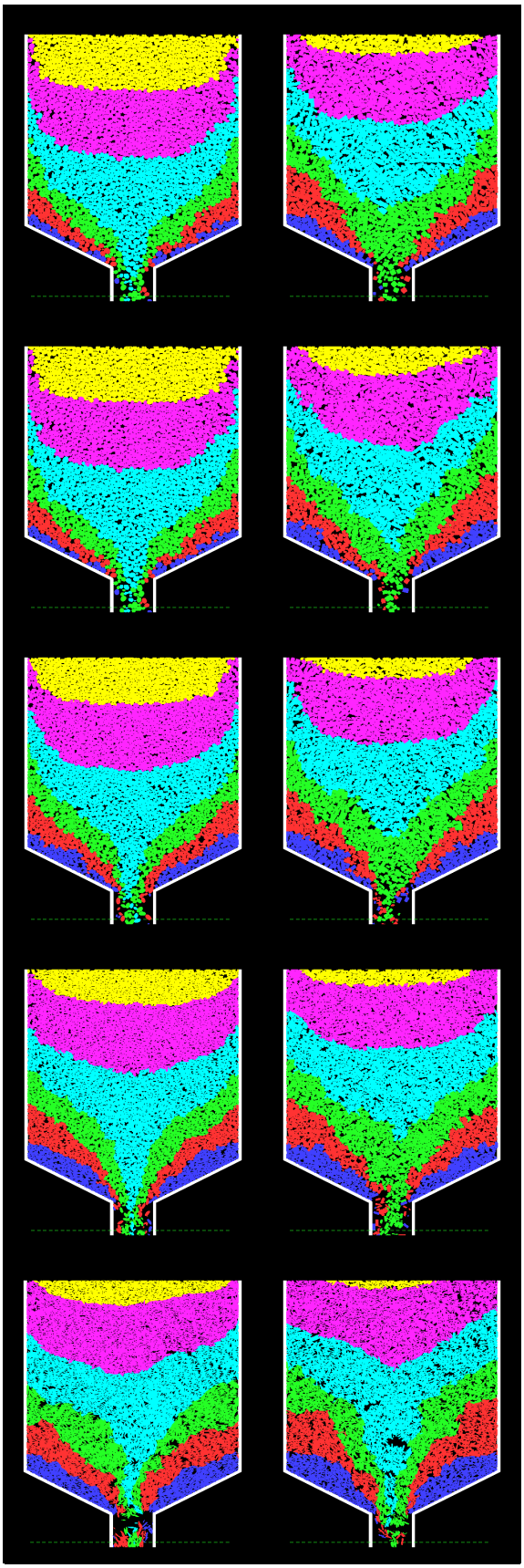

Figure 4: Discharge pattern for varying particle aspect ratio corresponding to rows (from top to bottom) A=1, A=0.8, A=0.6, A=0.4 and A=0.2**.** Circular particle cases on the left and rectangular (N=10) particles on the right.

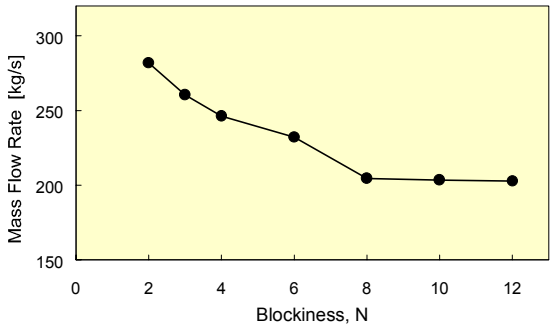

Figure 5: Mass flow rate from the hopper as a function of particle blockiness.

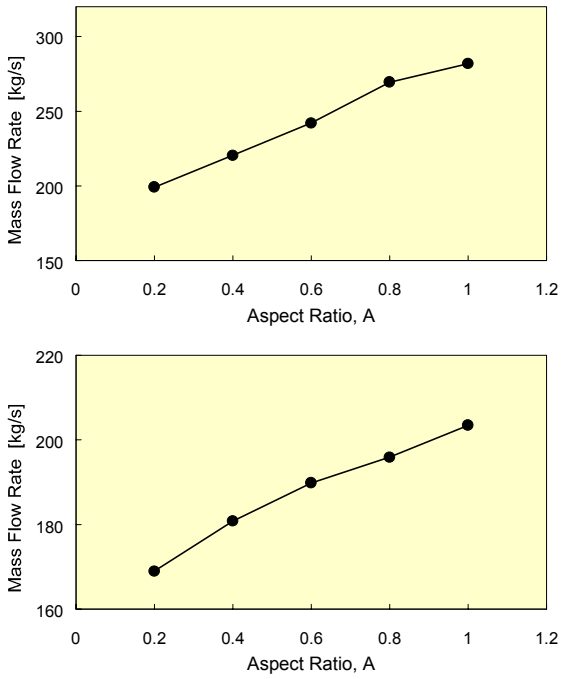

Figure 6: Variation of mass flow rate with aspect ratio for elliptical (top) and rectangular (bottom) particles.

There is a well-defined periodicity to these fluctuations with a frequency of approximately 7.8 Hz. This is clearly modulated by at least one much longer period oscillation. Close inspection of animations of these flows reveals the source of these fluctuations. The pressure from particles above pushes the particles adjacent to the wall both outwards and down. These particles are supported by friction with the walls as some contacts with particles below. As the hopper discharges and the particle microstructure below re-arranges itself, this lower support steadily diminishes. Eventually, the frictional forces on the walls exceed the Coulomb limits and all the unsupported particles fall abruptly until they come to rest on the particles below. This is known as a slip-stick phenomena and is responsible for silo quaking and honking. It can be clearly seen in the visualisations where large amounts of the upper material remains stationary for some time and then abruptly moves lower. The ability of DEM to predict this phenomena at least qualitatively is encouraging.

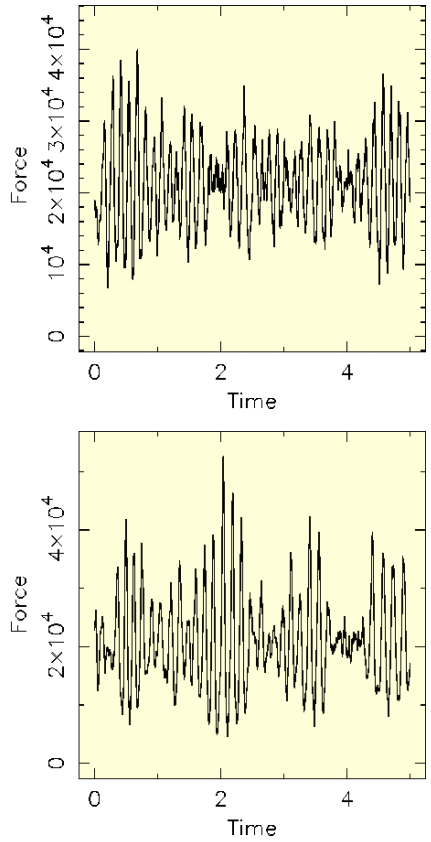

Figure 7: Vertical force (in N) applied to the walls of the hopper by circular particles (top), and rectangular particles (N=10, A=0.4) (bottom) as a function of time (in s).

Figure 7b shows the corresponding vertical wall force for elongated blocky material (N=10 and A=0.4). The time series is surprisingly similar with a clearly dominant frequency at around 7.6 Hz. The modulation of the primary frequency is somewhat different and the amplitude of the oscillations is slightly larger.

CONCLUSION

Hopper discharge has been modelled using DEM for a wide selection of particle shapes in order to ascertain the effect that shape has on the flow.

Circular particles are a particularly special case that do not represent well real materials. Circular particles have little resistance to shear or frictional forces. These forces cause the particle microstructure to yield prematurely via a rolling mode of failure. This causes the flow rates to be over-estimated and always leads to excessively fluid-like mass flow in the hoppers.

The effect of both particle aspect ratio and blockiness have been investigated independently and then together. The blockiness of the material surprisingly makes little difference to the actual pattern of the particle flow. Increasing blockiness does increase the resistance to flow and reduces the flow rate by around 28%, but the flow pattern is still closer to mass flow than to real funnel flow. The reduction in flow rate plateaus for N>8. The hopper flows are not sensitive to any further subtle increases in the angularity of the particles. This is quite different to the behaviour found for dragline bucket filling.

Increasing the aspect ratio of the particles has a stronger effect on the flow. The behavioural changes are similar for elliptical particles and for rectangular particles. Changing from circular particles to elliptical ones with a 5:1 aspect ratio (A=0.2) leads not only to a 29% reduction in the flow rate, but also substantial changes in the structure of the particle flow. These particles no longer behave as free-flowing independent particles but behave more like deforming, fracturing continua. Yielding leads to tearing of the microstructure fabric, leading to substantial voids that are quasi-stable and supported by arching stresses. A number of these cases also lead to spontaneous stable bridging. These particles essentially generate funnel flow.

Overall, particle shape is extremely important in hopper flows. This extension of DEM to use non-circular particles represents one amongst many important steps that are required before DEM can confidently predict all the phenomena that occur in hoppers. Other effects still to be understood include the locking of three-dimensional microstructures, the effect of particle asymmetry, the effect of cohesion, the effects of differing wall-particle to particle-particle friction properties and the effect of micro-roughness on the walls of the hopper.

REFERENCES

BARKER, G.C., 1994, "Computer simulations of granular materials", in *Granular Matter: An Inter-disciplinary Approach*, A. Mehta (ed.), Springer-Verlag.

CAMPBELL, C.S., 1990, "Rapid granular flows", *Ann. Rev. Fluid Mech.*, **22**, 57-92.

CLEARY, P.W., 1998a, "The filling of dragline buckets", *Math. Eng. in Indust.*, **7**, 1-24.

CLEARY, P.W., 1998b, "Predicting charge motion, power draw, segregation, wear and particle breakage in ball mills using discrete element methods", *Minerals Eng.*, **11**, 1061-1080.

CLEARY, P.W., 1998c, "Discrete element modelling of industrial granular flow applications", *TASK. Quarterly - Scientific Bulletin*, **2**, 385-416.

CLEARY, P.W., 1999, "DEM simulation of industrial particle flows: case studies of dragline excavators, mixing in tumblers and centrifugal mills", *To appear in Powder Tech*.

HOLST, J.M., ROTTE, J.M., OOI, J.Y. and RONG, G.H., 1997, "Discrete particle and continuum modelling of particulate solids in silos: SILO FILLING", *Research report R97-007, Dept. of Civil and Environmental Engineering, University of Edinburgh, Edinburgh, UK*

MISHRA, B.K. and RAJAMANI, R.K., 1992, "The discrete element method for the simulation of ball mills", *App. Math. Model.*, **16**, 598-604.

MISHRA, B.K. and RAJAMANI, R.K., 1994, "Simulation of charge motion in ball mills. Part 1: experimental verifications", *Int. J. Mineral Process.*, **40**, 171-186.

WALTON, O.R., 1994, "Numerical simulation of inelastic frictional particle-particle interaction", in *Particulate Two-Phase Flow*, M.C. Roco (ed.), Butterworth-Heineman, Chpt. 25, 884-911.

WILLIAMS, J.R. and PENTLAND, A., 1992, "Super-quadrics and modal dynamics for discrete elements in interactive design", *Int. J. Comp. Aided Eng. Software Eng. Comp.*, **9**, 115-127.